Scalable Total BETI based solver for 3D multibody frictionless contact problems in mechanical engineering

M. Sadowská[a,*], Z. Dostál[a], T. Kozubek[a], A. Markopoulos[a], J. Bouchala[a]

[a] *Department of Applied Mathematics*
VŠB – Technical University of Ostrava
17. listopadu 15, Ostrava, CZ-70833, Czech Republic

Abstract

A Total BETI (TBETI) based domain decomposition algorithm with the preconditioning by a natural coarse grid of the rigid body motions is adapted for the solution of multibody frictionless contact problems of linear elastostatics and proved to be scalable, i.e., the cost of the solution is asymptotically proportional to the number of variables. The analysis admits floating bodies. The proofs combine the original results by Langer and Steinbach on the scalability of BETI for linear problems and our development of optimal quadratic programming algorithms for bound and equality constrained problems. The theoretical results are verified by numerical experiments. The power of the method is demonstrated on the analysis of ball bearings.

Keywords: Boundary elements, multibody contact problems, domain decomposition, BETI, scalability, floating bodies

1. Introduction

The contact of one body with another is a typical way how loads are delivered to a structure and at the same time it is the mechanism which supports structures to sustain the loads. Thus we do not exaggerate much if we say that the contact problems are in the heart of mechanical engineering. Solving large multibody contact problems of linear elastostatics is complicated by the inequality boundary conditions, which make them strongly non-linear, and, if the system of bodies includes "floating" bodies, by the positive semi-definite stiffness matrices resulting from the discretization of such bodies. Observing that the classical Dirichlet and Neumann boundary

*Corresponding author.
Email address: marie.sadowska@vsb.cz (M. Sadowská)

conditions are known only after the solution has been found, it is natural to assume the solution of contact problems to be more costly than the solution of a related linear problem with the classical boundary conditions. Since the cost of the solution of any problem increases at least linearly with the number of the unknowns, it follows that the development of a scalable algorithm for contact problems is a challenging task which requires to identify the contact interface in a sense for free. Let us recall that an algorithm is *numerically scalable* if the cost of the solution increases nearly proportionally to the number of unknown variables, and it enjoys the *parallel scalability* if the cost of the solution can be reduced nearly proportionally to the number of available processors. Scalable algorithms are also called optimal.

In spite of this, there has been made a considerable effort in this direction and a number of interesting results have been obtained. Most of the results, either experimental or theoretical, were obtained for the problems discretized by the Finite Element Method (FEM), either in the framework of the domain decomposition methods, see, e.g., Schöberl [42], Dureisseix and Farhat [22], Avery et al. [1], Avery and Farhat [2], or by the multigrid methods, see, e.g., Kornhuber [34], Kornhuber and Krause [35], and Wohlmuth and Krause [54]. Most recently, a theoretically supported scalable algorithm for both coercive and semi-coercive contact problems was presented by Dostál et al. [16].

A number of researchers developed effective algorithms also for the solution of contact problems by Boundary Element Method (BEM), including problems with friction [23], problems discretized by mortars [43], or semi-coercive problems [15]. The main benefit of the application of the BEM, as compared with the more popular FEM, is that the formulation of the problem is reduced to the boundary of the underlying domain which yields a significant dimension reduction. In particular, BEM is desirable, e.g., when dealing with large or unbounded domains [39] or shape optimization problems [9]. However, since BEM requires the explicit knowledge of a fundamental solution of a given partial differential operator, it is applicable only to the problems involving materials with rather simple properties.

The activity in the development of optimal algorithms for contact problems discretized by BEM lagged behind the related FEM research. This is rather surprising, since BEM seems to be a suitable tool for treating the non-linearity which is restricted to the contact interface. The reason for such a delay is that a suitable boundary element domain decomposition method, BETI (Boundary Element Tearing and Interconnection), was introduced by Langer and Steinbach [38] only in 2003, much later than Farhat and Roux [26] proposed their FETI (Finite Element Tearing and Interconnecting) method, and, as observed by Iontcheva and Vassilevski [32], that the convergence of the multigrid method for contact problems requires to keep

the coarse grid away from the contact interface. Thus it seems that the first scalability results, first for the scalar variational inequalities and later for the coercive contact problems, were presented only recently by Bouchala, Dostál, and Sadowská [6, 5]. The theory was illustrated on a problem of academic interest.

The point of this paper is to extend these results to the solution of the semi-coercive multibody contact problems with "floating" bodies and to demonstrate the efficiency of our algorithms on the solution of realistic problems. In particular, we show how to modify our optimal algorithm for coercive problems [5] so that the optimality results remain valid for semi-coercive problems. Let us point out that we have in mind optimality in a very specific sense. In particular, our theory assumes that the problem is decomposed into subdomains with a number of variables bounded independently on the discretization parameter. Since the Hessian of the resulting quadratic problem is in this case block-diagonal with the blocks of nearly the same order, the cost of the matrix–vector multiplications is in this particular case proportional to the number of variables. We use the direct approach, which reformulates the boundary value problem in terms of the Boundary Integral Equations (BIEs) and the unknown Cauchy data (trace of the solution and its corresponding conormal derivative) are found by solving these BIEs. We combine the direct method with the Galerkin discretization; though we have to handle double boundary integrals instead of a single boundary integration that arises from the application of the collocation method, we get the stiffness matrices that are closely related to the Schur complements of the matrices arising from FEM.

Our main tools are our in a sense optimal quadratic programming algorithms [12] and the Boundary Element Tearing and Interconnecting (BETI) method – a combination of the symmetric Galerkin BEM with the duality based Domain Decomposition (DD) approach – as it was originally introduced by Langer and Steinbach [38]. The essential idea behind DD methods is splitting the original boundary value problem into local problems on smaller subdomains that decompose the underlying domains which correspond to the bodies involved in the problem. The local problems are then coupled by suitable transmission conditions introduced on the artificial interfaces between subdomains. We use the "All Floating" or "Total" variant of the BETI method introduced independently by Of [44, 45] and Dostál, Horák, and Kučera [20], respectively. This approach enforces the Dirichlet boundary conditions by additional Lagrange multipliers, so that the kernels of the stiffness matrices of all the subdomains are a priori known. After the application of duality, we employ preconditioning by the projectors to the so-called natural coarse grid that was originally proposed by Farhat et al. [25] for preconditioning of their FETI method. Since Langer and Steinbach showed in [38] that the discrete approximate Steklov–Poincaré operators

generated by the FETI and BETI methods are spectrally equivalent, we can exploit the analysis of Farhat et al. [25] to get the bounds on the spectrum of the preconditioned dual stiffness matrix independent of the discretization and decomposition parameters h and H, respectively. Let us point out that although our method is based on that introduced by Langer and Steinbach [38], we cannot use their preconditioning strategy, since their preconditioner transforms the bound constraints into more general inequalities, which prevents the application of our optimal algorithms.

The paper is organized as follows. In Section 2, we review some basic results concerning boundary integral operators. The continuous frictionless multibody contact problem is introduced in Section 3. In Section 4, we apply the non-overlapping domain decomposition and briefly review the variational formulation of our problem. In Section 5, we introduce the bound and equality constrained dual problem whose conditioning is further improved in Section 6 by using the projectors to the natural coarse grid. In Section 7, we review our algorithms for the solution of the resulting quadratic programming problem with bound and equality constraints whose rate of convergence can be expressed in terms of bounds on the spectrum of the preconditioned dual stiffness matrix [13, 21, 12]. Section 8 presents the main results about optimality of our method. In Section 9, we give results of numerical experiments which are in a good agreement with the theory and demonstrate the scalability of the presented method. We demonstrate the power of our algorithm on the solution of a real world problem. Finally, in Section 10, we give some comments and remarks concerning the possibilities of the future extension of our method.

2. Dirichlet–Neumann map for 3D linear homogeneous isotropic elastostatics

To facilitate our presentation, we start with a brief review of some well-known results concerning boundary integral operators. For more details, see, e.g., [10, 40, 52, 47].

Let $\Omega \subset \mathbb{R}^3$ be a bounded Lipschitz domain with the boundary Γ that is filled with a homogeneous isotropic material. We consider the elliptic partial differential operator $\mathcal{L}$ defined by

$$(\mathcal{L}\underline{u})_i(x) := -\sum_{j=1}^{3} \frac{\partial}{\partial x_j}\sigma_{ij}(\underline{u}, x) \quad \text{for } x \in \Omega,\ i = 1, 2, 3,$$

where the stress tensor σ is given by the Hooke law

$$\sigma_{ij}(\underline{u}, x) := \frac{E\nu}{(1+\nu)(1-2\nu)}\delta_{ij}\sum_{k=1}^{3} e_{kk}(\underline{u}, x) + \frac{E}{1+\nu}e_{ij}(\underline{u}, x) \quad \text{for } i, j = 1, 2, 3$$

with the strain tensor e defined by

$$e_{ij}(\underline{u}, x) := \frac{1}{2}\left(\frac{\partial}{\partial x_i}u_j(x) + \frac{\partial}{\partial x_j}u_i(x)\right) \quad \text{for } i, j = 1, 2, 3,$$

Young's modulus $E > 0$, and Poisson's ratio $\nu \in (0, 1/2)$. Both E and ν are assumed to be constant.

Now let us introduce the standard interior trace and boundary traction operators

$$\gamma_0 : \ [H^1(\Omega)]^3 \mapsto [H^{1/2}(\Gamma)]^3 \quad \text{and} \quad \gamma_1 : \ [H^1_{\mathcal{L}}(\Omega)]^3 \mapsto [H^{-1/2}(\Gamma)]^3,$$

respectively, where $H^{1/2}(\Gamma)$ is the trace space of $H^1(\Omega)$, $H^{-1/2}(\Gamma)$ is the dual space to $H^{1/2}(\Gamma)$ with respect to the $L^2(\Gamma)$ scalar product, and

$$[H^1_{\mathcal{L}}(\Omega)]^3 := \left\{\underline{v} \in [H^1(\Omega)]^3 : \ \mathcal{L}\underline{v} \in [L^2(\Omega)]^3\right\}.$$

Recall that for all $\underline{v} \in [C^\infty(\overline{\Omega})]^3$ and $i = 1, 2, 3$

$$(\gamma_0\underline{v})_i(x) = v_i(x) \quad \text{and} \quad (\gamma_1\underline{v})_i(x) = \sum_{j=1}^{3} \sigma_{ij}(\underline{v}, x)\, n_j(x) \quad \text{for } x \in \Gamma$$

with $n_j(x)$ denoting jth component of the outer unit normal vector $\underline{n}(x)$ that is defined for almost all $x \in \Gamma$.

The fundamental solution U of the operator $\mathcal{L}$ is called Kelvin's tensor and is given for any distinct $x, y \in \mathbb{R}^3$ and $i, j = 1, 2, 3$ by

$$U_{ij}(x, y) := \frac{1+\nu}{8\pi E(1-\nu)}\left((3-4\nu)\frac{\delta_{ij}}{\|x-y\|} + \frac{(x_i - y_i)(x_j - y_j)}{\|x-y\|^3}\right).$$

Moreover, let us denote $\underline{U}_j := (U_{1j}, U_{2j}, U_{3j})$. It is well-known [52, 47, 23] that any function $\underline{u} \in [H^1_{\mathcal{L}}(\Omega)]^3$ can be represented via Somigliana's identity as

$$u_j(x) = \int_\Gamma \big(\gamma_1\underline{u}(y),\, \underline{U}_j(x, y)\big)\, \mathrm{d}s_y - \int_\Gamma \big(\gamma_0\underline{u}(y),\, \gamma_{1,y}\underline{U}_j(x, y)\big)\, \mathrm{d}s_y + \\ + \int_\Omega \big(\mathcal{L}\underline{u}(y),\, \underline{U}_j(x, y)\big)\, \mathrm{d}y \tag{1}$$

for $x \in \Omega$ and $j = 1, 2, 3$, where $(\cdot, \cdot)$ denotes the Euclidean scalar product.

Applying the operators γ_0 and γ_1 to the Somigliana identity (1) and obeying the corresponding jump relations [52], we can derive the Dirichlet–Neumann map

$$\gamma_1\underline{u}(x) = (S\gamma_0\underline{u})(x) - (N\mathcal{L}\underline{u})(x) \quad \text{for } x \in \Gamma$$

with the Steklov–Poincaré operator

$$S := (\sigma I + K')V^{-1}(\sigma I + K) + D : \ [H^{1/2}(\Gamma)]^3 \mapsto [H^{-1/2}(\Gamma)]^3, \tag{2}$$

where $\sigma(x) = 1/2$ for almost all $x \in \Gamma$, and the Newton operator

$$N := V^{-1}N_0 : \ [L^2(\Omega)]^3 \mapsto [H^{-1/2}(\Gamma)]^3. \tag{3}$$

In (2) and (3) we use the single layer potential operator V, double layer potential operator K, adjoint double layer potential operator K', hypersingular integral operator D given for $x \in \Gamma$ and $i = 1, 2, 3$ by

$$\begin{aligned}
(V\underline{t})_i(x) &:= \int_\Gamma (\underline{t}(y),\, \underline{U}_i(x,y))\ \mathrm{d}s_y, && V : \ [H^{-1/2}(\Gamma)]^3 \mapsto [H^{1/2}(\Gamma)]^3,\\
(K\underline{u})_i(x) &:= \int_\Gamma (\underline{u}(y),\, \gamma_{1,y}\underline{U}_i(x,y))\ \mathrm{d}s_y, && K : \ [H^{1/2}(\Gamma)]^3 \mapsto [H^{1/2}(\Gamma)]^3,\\
(K'\underline{t})_i(x) &:= \int_\Gamma (\underline{t}(y),\, \gamma_{1,x}\underline{U}_i(x,y))\ \mathrm{d}s_y, && K' : \ [H^{-1/2}(\Gamma)]^3 \mapsto [H^{-1/2}(\Gamma)]^3,\\
(D\underline{u})_i(x) &:= -\gamma_{1,x}\int_\Gamma (\underline{u}(y),\, \gamma_{1,y}\underline{U}_i(x,y))\ \mathrm{d}s_y, && D : \ [H^{1/2}(\Gamma)]^3 \mapsto [H^{-1/2}(\Gamma)]^3,
\end{aligned}$$

and the Newton potential operator N_0 given for $x \in \Gamma$ and $i = 1, 2, 3$ by

$$(N_0\underline{f})_i(x) := \int_\Omega (\underline{f}(y),\, \underline{U}_i(x,y))\ \mathrm{d}y, \qquad N_0 : \ [L^2(\Omega)]^3 \mapsto [H^{1/2}(\Gamma)]^3.$$

The mapping properties of the above integral operators are well-known [10, 52], in particular, the single layer potential operator is $[H^{-1/2}(\Gamma)]^3$–elliptic, so that its inversion is well-defined. Finally, let us state the following two lemmas:

Lemma 2.1 [52] *The Steklov–Poincaré operator S is linear, bounded, symmetric, and semi-elliptic on $[H^{1/2}(\Gamma)]^3$. Moreover, if Γ_d is a subset of Γ with $\mathrm{meas}\,\Gamma_d > 0$ and $H_0^{1/2}(\Gamma, \Gamma_d) := \{v \in H^{1/2}(\Gamma) : \ v(x) = 0 \text{ for } x \in \Gamma_d\}$, then S is elliptic on $[H_0^{1/2}(\Gamma, \Gamma_d)]^3$. The kernel of S is equal to the space of the rigid body motions, i.e.,*

$$\mathrm{Ker}\, S = \mathrm{span}\left\{ \begin{pmatrix} 1 \\ 0 \\ 0 \end{pmatrix}, \begin{pmatrix} 0 \\ 1 \\ 0 \end{pmatrix}, \begin{pmatrix} 0 \\ 0 \\ 1 \end{pmatrix}, \begin{pmatrix} -x_2 \\ x_1 \\ 0 \end{pmatrix}, \begin{pmatrix} 0 \\ -x_3 \\ x_2 \end{pmatrix}, \begin{pmatrix} x_3 \\ 0 \\ -x_1 \end{pmatrix} \right\}.$$

Lemma 2.2 [52] *The Newton operator N is linear and bounded on $[L^2(\Omega)]^3$.*

3. Frictionless multibody contact problem

To simplify our presentation, we restrict our attention to the case of contact problems without friction, but the theoretical background following in the next sections can be extended also to problems with the Tresca and Coulomb friction [17, 18]. We shall discuss this point in a forthcoming paper.

Let us consider a system of s homogeneous isotropic elastic bodies whose reference configurations occupy bounded Lipschitz domains

$$\Omega^p \subset \mathbb{R}^3, \quad p = 1, 2, \ldots, s$$

with the boundaries

$$\Gamma^p := \partial\Omega^p, \quad p = 1, 2, \ldots, s,$$

each of which comprises three non-overlapping parts

$$\Gamma_d^p, \ \Gamma_n^p, \ \text{and} \ \Gamma_c^p, \quad p = 1, 2, \ldots, s,$$

denoting the Dirichlet, Neumann, and contact boundary of the pth body, respectively. In particular, we denote by Γ_c^{pq} a part of Γ_c^p, which is allowed to be in contact with the body Ω^q. The mechanical properties of Ω^p are characterized by the Young modulus $E^p > 0$ and the Poisson ratio $\nu^p \in (0, 1/2)$. These material parameters are assumed to be constant for each Ω^p. An example of a reference configuration of a two-body contact problem can be seen in Figure 1.

To enhance the contact with rigid obstacles, we admit the bodies with a priori defined zero displacements on the whole boundary (see Figure 2).

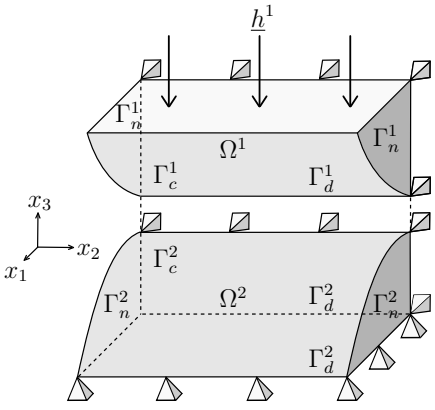

Figure 1: A two-body contact problem.

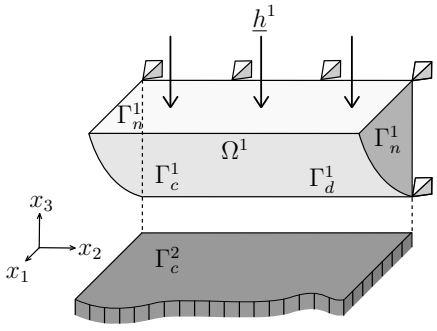

Figure 2: A contact problem with rigid obstacle.

In what follows, we denote by $\underline{u}^p : \Gamma^p \mapsto \mathbb{R}^3$ the boundary displacements corresponding to the pth body. Moreover, the imposed boundary displacements, boundary traction, and the volume forces acting inside the body Ω^p are denoted by

$$\underline{g}^p \in [H^{1/2}(\Gamma_d^p)]^3, \quad \underline{h}^p \in [L^2(\Gamma_n^p)]^3, \quad \text{and} \quad \underline{f}^p \in [L^2(\Omega^p)]^3,$$

respectively.

In order to describe the linearized non-interpenetration conditions, let us define for each $p < q$ and $\Gamma_c^{pq} \neq \emptyset$ a one-to-one continuous mapping

$$\underline{\mathcal{O}}^{pq} : \Gamma_c^{pq} \mapsto \Gamma_c^{qp},$$

so that $\underline{\mathcal{O}}^{pq}(x) \in \Gamma_c^{qp}$ is a "near" point to $x \in \Gamma_c^{pq}$. Now for each $p < q$ the linearized non-interpenetration condition is defined by

$$(\underline{u}^p(x) - \underline{u}^q(\underline{\mathcal{O}}^{pq}(x)), \underline{n}^p(x)) \leq (\underline{\mathcal{O}}^{pq}(x) - x, \underline{n}^p(x)) \quad \text{for } x \in \Gamma_c^{pq}, \tag{4}$$

where $\underline{n}^p(x)$ is the outer unit normal vector to Ω^p at x; see Figure 3. For more details, see also [33, 55].

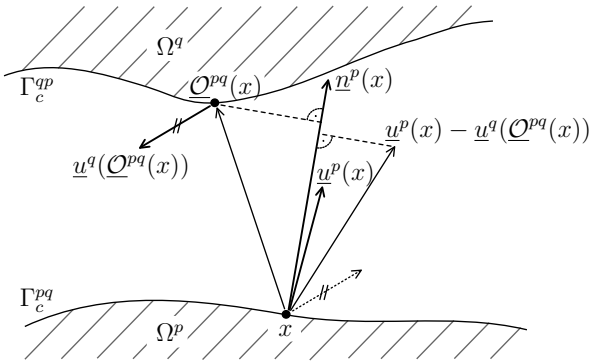

Figure 3: The linearized non-interpenetration in 2D.

Let us introduce the Sobolev product space

$$\mathcal{V} := [H^{1/2}(\Gamma^1)]^3 \times \cdots \times [H^{1/2}(\Gamma^s)]^3$$

equipped with the norm

$$\|\underline{v}\|_{\mathcal{V}} := \left(\sum_{p=1}^{s} \|\underline{v}^p\|^2_{[H^{1/2}(\Gamma^p)]^3} \right)^{1/2} \quad \text{for } \underline{v} = (\underline{v}^1, \ldots, \underline{v}^s) \in \mathcal{V}.$$

For any displacement $\underline{u} = (\underline{u}^1, \ldots, \underline{u}^s) \in \mathcal{V}$ let us define the so-called energy functional by

$$\mathcal{J}(\underline{u}) = \frac{1}{2}\mathcal{A}(\underline{u}, \underline{u}) - \mathcal{F}(\underline{u}),$$

where $\mathcal{A}$ is a bilinear form on $\mathcal{V}$ defined by

$$\mathcal{A}(\underline{u}, \underline{v}) := \sum_{p=1}^{s} \langle S^p \underline{u}^p, \underline{v}^p \rangle_{\Gamma^p}$$

and $\mathcal{F}$ is a linear functional on $\mathcal{V}$ given by

$$\mathcal{F}(\underline{v}) := \sum_{p=1}^{s} \left\{ \langle N^p \underline{f}^p, \underline{v}^p \rangle_{\Gamma^p} + \langle \underline{h}^p, \underline{v}^p \rangle_{\Gamma_n^p} \right\}$$

with

$$\langle \underline{w}, \underline{y} \rangle_{\Gamma^p} := \sum_{i=1}^{3} \langle w_i, y_i \rangle_{L^2(\Gamma^p)} .$$

By

$$S^p : \ [H^{1/2}(\Gamma^p)]^3 \mapsto [H^{-1/2}(\Gamma^p)]^3 \quad \text{and} \quad N^p : \ [L^2(\Omega^p)]^3 \mapsto [H^{-1/2}(\Gamma^p)]^3$$

we denote the Steklov–Poincaré and Newton operators, respectively, whose properties are briefly discussed in the previous section. Furthermore, let

$$\mathcal{K}_d := \left\{ \underline{v} = (\underline{v}^1, \ldots, \underline{v}^s) \in \mathcal{V} : \ \underline{v}^p = \underline{g}^p \quad \text{on } \Gamma_d^p \quad \text{for } p = 1, \ldots, s \right\},$$

$$\mathcal{K}_c := \Big\{ \underline{v} = (\underline{v}^1, \ldots, \underline{v}^s) \in \mathcal{V} : \ (\underline{v}^p(x) - \underline{v}^q(\underline{\mathcal{O}}^{pq}(x)), \underline{n}^p(x)) \ \leq \ (\underline{\mathcal{O}}^{pq}(x) - x, \underline{n}^p(x)) \quad \text{for } x \in \Gamma_c^{pq}, \ p, q = 1, \ldots, s, \ \text{and } p < q \Big\},$$

and

$$\mathcal{K} := \mathcal{K}_d \cap \mathcal{K}_c.$$

Note that $\mathcal{K}$ is a non-empty, closed, and convex subset of $\mathcal{V}$.

A potential energy minimization problem now reads: find the displacement $\underline{u} \in \mathcal{K}$ such that

$$\mathcal{J}(\underline{u}) = \min\{\mathcal{J}(\underline{v}) : \ \underline{v} \in \mathcal{K}\}. \tag{5}$$

Due to Lemmas 2.1 and 2.2, the bilinear form $\mathcal{A}$ is bounded, symmetric, and semi-elliptic on $\mathcal{V}$ and the linear functional $\mathcal{F}$ is bounded on $\mathcal{V}$. Thus the energy functional $\mathcal{J}$ is continuous and convex on $\mathcal{V}$. The remaining conditions that guarantee the

existence and uniqueness of the solution of (5), in particular, the coercivity of $\mathcal{J}$ on $\mathcal{K}$, may be found, for instance, in [31, 33].

Finally, let us note that more general boundary conditions, such as prescribed normal displacements and zero forces in the tangential plane, may be also considered without any conceptual difficulties.

4. Total BETI (TBETI) domain decomposition and discretization

In order to develop a method suitable for the efficient parallel solution of our model problem, let us first "tear" each body from the part of the boundary with the Dirichlet boundary condition, and then decompose each body into non-overlapping Lipschitz subdomains, assign each subdomain a unique number, and introduce new "gluing" conditions on the artificial intersubdomain boundaries and on the boundaries with imposed Dirichlet condition. Analogously to the notation of the contact boundaries Γ_c^p and Γ_c^{pq}, let Γ_g^p and Γ_g^{pq} denote the part of Γ^p that is glued to the other subdomains and the part of Γ^p that is glued to Ω^q, respectively. A decomposition of the problem in Figure 2 with renumbered subdomains and artificial intersubdomain boundaries is depicted in Figure 4. The gluing conditions require continuity of the boundary displacements and boundary traction across the intersubdomain boundaries. Let us note that by s we still mean the number of all bodies, i.e., s is equal to the number of all subdomains after decomposition.

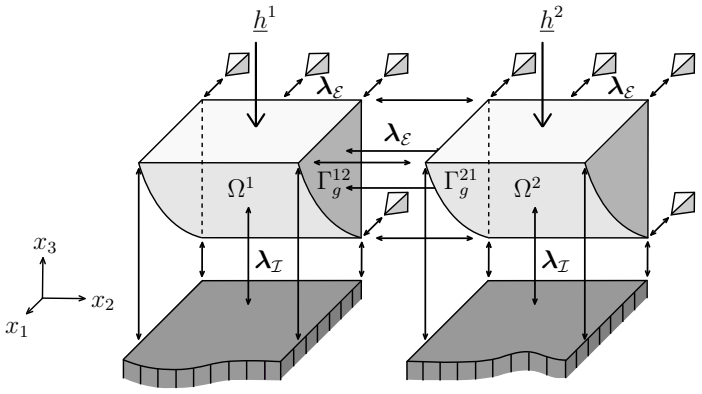

Figure 4: TBETI domain decomposition of the problem in Figure 2 with renumbering.

Before we arrive at the discrete formulation of our decomposed problem, we first have to mention the approximations $\widetilde{S}^p$ and $\widetilde{N}^p$ of the Steklov–Poincaré and Newton

operators S^p and N^p, respectively, in order to avoid their implicit representations due to the inversion of the single layer operator (see (2), (3)). We approximate both operators by using the boundary element method with piecewise constant trial functions ψ_k^p, $k = 1, \ldots, L^p$, $p = 1, \ldots, s$, as it is described, e.g., in [51, 38], so that such approximations preserve all properties stated in Lemmas 2.1 and 2.2.

In the following, we use the symbols $\mathcal{I}$ and $\mathcal{E}$ to distinguish between the sets of indices corresponding to the inequalities and equalities, respectively. The boundary element discretization of $\Gamma^1, \ldots, \Gamma^s$ with piecewise linear trial functions φ_ℓ^p, $\ell = 1, \ldots, M^p$, $p = 1, \ldots, s$, results in the quadratic programming problem

$$\text{minimize} \quad J(\mathbf{v}) \quad \text{subject to} \quad \mathsf{B}_{\mathcal{I}}\mathbf{v} \le \mathbf{c}_{\mathcal{I}} \quad \text{and} \quad \mathsf{B}_{\mathcal{E}}\mathbf{v} = \mathbf{c}_{\mathcal{E}}, \tag{6}$$

where

$$J(\mathbf{v}) := \frac{1}{2}\mathbf{v}^\top \widetilde{\mathsf{S}}\mathbf{v} - \widetilde{\mathbf{r}}^\top \mathbf{v},$$

$$\widetilde{\mathsf{S}} := \begin{pmatrix} \widetilde{\mathsf{S}}_1 & \mathsf{O} & \mathsf{O} \\ \mathsf{O} & \ddots & \mathsf{O} \\ \mathsf{O} & \mathsf{O} & \widetilde{\mathsf{S}}_s \end{pmatrix}, \quad \mathbf{v} := \begin{pmatrix} \mathbf{v}_1 \\ \vdots \\ \mathbf{v}_s \end{pmatrix}, \quad \mathbf{v}_p := \begin{pmatrix} \mathbf{v}_{p,1} \\ \mathbf{v}_{p,2} \\ \mathbf{v}_{p,3} \end{pmatrix}, \quad \widetilde{\mathbf{r}} := \begin{pmatrix} \widetilde{\mathbf{r}}_1 \\ \vdots \\ \widetilde{\mathbf{r}}_s \end{pmatrix}. \tag{7}$$

Here, $\widetilde{\mathsf{S}}_p \in \mathbb{R}^{3M^p \times 3M^p}$ denotes the discrete approximate Steklov–Poincaré operator

$$\widetilde{\mathsf{S}}_p := \mathsf{D}_p + (\frac{1}{2}\mathsf{M}_p + \mathsf{K}_p)^\top \mathsf{V}_p^{-1} (\frac{1}{2}\mathsf{M}_p + \mathsf{K}_p)$$

and $\widetilde{\mathbf{r}}_p \in \mathbb{R}^{3M^p}$ denotes the discrete approximate Newton operator

$$\widetilde{\mathbf{r}}_p := \mathsf{M}_p^\top \left(\mathsf{V}_p^{-1} \mathbf{N}_{0,p} + \widehat{\mathbf{h}}_p \right).$$

Note that the boundary element matrices V_p, K_p, and D_p are all fully populated. Moreover, matrices V_p and D_p are symmetric positive definite and semi-definite, respectively. We consider the same boundary meshes corresponding to the discretizations by piecewise constant and piecewise linear trial functions ψ_k^p and φ_ℓ^p, respectively, with the plane triangles denoted by τ_k^p, $k = 1, \ldots, L^p$, $p = 1, \ldots, s$.

For the discrete single layer potential operator there holds the representation [47, 52]

$$\mathsf{V}_p = \frac{1+\nu^p}{2E^p(1-\nu^p)} \left((3-4\nu^p) \begin{pmatrix} \mathsf{V}_p^{\triangle} & \mathsf{O} & \mathsf{O} \\ \mathsf{O} & \mathsf{V}_p^{\triangle} & \mathsf{O} \\ \mathsf{O} & \mathsf{O} & \mathsf{V}_p^{\triangle} \end{pmatrix} + \begin{pmatrix} \mathsf{V}_{11,p} & \mathsf{V}_{12,p} & \mathsf{V}_{13,p} \\ \mathsf{V}_{12,p} & \mathsf{V}_{22,p} & \mathsf{V}_{23,p} \\ \mathsf{V}_{13,p} & \mathsf{V}_{23,p} & \mathsf{V}_{33,p} \end{pmatrix} \right)$$

with the discrete single layer potential operator $\mathsf{V}_p^{\triangle} \in \mathbb{R}^{L^p \times L^p}$ for the Laplace operator defined by

$$\mathsf{V}_p^{\triangle}[k,\ell] := \frac{1}{4\pi} \int_{\tau_k^p} \int_{\tau_\ell^p} \frac{1}{\|x-y\|} \,\mathrm{d}s_y \,\mathrm{d}s_x$$

and the matrices $\mathsf{V}_{ij,p} \in \mathbb{R}^{L^p \times L^p}$ defined by

$$\mathsf{V}_{ij,p}[k,\ell] := \frac{1}{4\pi} \int_{\tau_k^p} \int_{\tau_\ell^p} \frac{(x_i - y_i)(x_j - y_j)}{\|x-y\|^3} \,\mathrm{d}s_y \,\mathrm{d}s_x$$

for $k, \ell = 1, \ldots, L^p$, $i, j = 1, 2, 3$, $i \le j$.

For the discrete double layer potential operator there holds the representation [37, 47, 52]

$$\mathsf{K}_p = \begin{pmatrix} \mathsf{K}_p^{\triangle} & \mathsf{O} & \mathsf{O} \\ \mathsf{O} & \mathsf{K}_p^{\triangle} & \mathsf{O} \\ \mathsf{O} & \mathsf{O} & \mathsf{K}_p^{\triangle} \end{pmatrix} - \begin{pmatrix} \mathsf{V}_p^{\triangle} & \mathsf{O} & \mathsf{O} \\ \mathsf{O} & \mathsf{V}_p^{\triangle} & \mathsf{O} \\ \mathsf{O} & \mathsf{O} & \mathsf{V}_p^{\triangle} \end{pmatrix} \mathsf{T}_p + \frac{E^p}{1+\nu^p} \mathsf{V}_p \mathsf{T}_p$$

with the discrete double layer potential operator $\mathsf{K}_p^{\triangle} \in \mathbb{R}^{L^p \times M^p}$ for the Laplace operator defined by

$$\mathsf{K}_p^{\triangle}[k,n] := \frac{1}{4\pi} \int_{\tau_k^p} \int_{\Gamma^p} \frac{(x-y,\, \underline{n}^p(y))}{\|x-y\|^3} \varphi_n^p(y) \,\mathrm{d}s_y \,\mathrm{d}s_x$$

and the sparse transformation matrix

$$\mathsf{T}_p := \begin{pmatrix} \mathsf{O} & \mathsf{T}_{12,p} & \mathsf{T}_{13,p} \\ -\mathsf{T}_{12,p} & \mathsf{O} & \mathsf{T}_{23,p} \\ -\mathsf{T}_{13,p} & -\mathsf{T}_{23,p} & \mathsf{O} \end{pmatrix},$$

where the blocks $\mathsf{T}_{ij,p} \in \mathbb{R}^{L^p \times M^p}$ are defined by

$$\mathsf{T}_{ij,p}[k,n] := n_j^p(x) \frac{\partial \varphi_n^p}{\partial x_i}(x) - n_i^p(x) \frac{\partial \varphi_n^p}{\partial x_j}(x), \quad x \in \tau_k^p,$$

for $k = 1, \ldots, L^p$, $n = 1, \ldots, M^p$, $i, j = 1, 2, 3$, $i < j$.

Entries of the matrices $\mathsf{V}_p^{\triangle}$, $\mathsf{V}_{ij,p}$, and $\mathsf{K}_p^{\triangle}$ may be calculated so that the inner integral is evaluated analytically and the outer one is approximated by using a suitable numerical scheme, as shown by Rjasanow and Steinbach in [47]. Another possibility how to evaluate the entries is to use the quadrature formulae based on

the Duffy transformation which removes the kernel singularity, as shown by Sauter and Schwab in [49]. To avoid the drawback of these conventional approaches, when we have to evaluate all entries of the full matrices, especially when their size becomes large (i.e., starting at thousands of unknows), one can exploit the so-called fast techniques such as Adaptive Cross Approximation (ACA) [4, 3] or Fast Multipole Method [29, 28, 46, 41] which accelerate the evaluation of the matrices and the consequent matrix–vector multiplication.

For the discrete hypersingular integral operator D_p there is a representation based on the transformation matrix T_p and the matrices $\mathsf{V}_p^{\triangle}$ and V_p, see [30, 47, 48].

Finally, the mass matrix M_p has the form

$$\mathsf{M}_p = \begin{pmatrix} \mathsf{M}_p^{\triangle} & \mathsf{O} & \mathsf{O} \\ \mathsf{O} & \mathsf{M}_p^{\triangle} & \mathsf{O} \\ \mathsf{O} & \mathsf{O} & \mathsf{M}_p^{\triangle} \end{pmatrix}$$

with $\mathsf{M}_p^{\triangle} \in \mathbb{R}^{L^p \times M^p}$ defined by

$$\mathsf{M}_p^{\triangle}[k,n] := \int_{\tau_k^p} \varphi_n^p(x)\,\mathrm{d}s_x$$

for $k = 1, \ldots, L^p$ and $n = 1, \ldots, M^p$.

The entries of the vector $\mathbf{N}_{0,p} \in \mathbb{R}^{3L^p}$ are given by

$$\mathbf{N}_{0,p,(i-1)L^p+k} := \langle (N_{0,p}\underline{f}^p)_i,\, \psi_k^p \rangle_{L^2(\Gamma^p)}$$

for $k = 1, \ldots, L^p$ and $i = 1, 2, 3$. The evaluation of $N_{0,p}\underline{f}^p$ may be done by using an indirect approach, as it is introduced in [50, 51]. Another possibility is the direct evaluation of $N_{0,p}\underline{f}^p$ requiring, however, a 3D mesh of Ω^p.

Let us consider the zero extension $\widehat{h}^p$ of the imposed boundary traction h^p from Γ_n^p to Γ^p and approximate $\widehat{h}^p$ by the piecewise constants ψ_k^p. The element values of the approximated $\widehat{h}^p$ then correspond to the entries of the vector $\widehat{\mathbf{h}}_p \in \mathbb{R}^{3L^p}$.

It remains to describe the constraining matrices and vectors arising in (6). First, note that both matrices $\mathsf{B}_{\mathcal{I}}$ and $\mathsf{B}_{\mathcal{E}}$ are constructed as the full rank ones. The matrix $\mathsf{B}_{\mathcal{I}}$ and the vector $\mathbf{c}_{\mathcal{I}}$ correspond to the linearized non-interpenetration conditions. The rows $\mathbf{b}_{\mathcal{I},i}$ of $\mathsf{B}_{\mathcal{I}}$ are formed by zeros and appropriately placed multiples of coordinates of the outer unit normals, so that the change of the normal distance due to the displacement $\mathbf{v}$ is given by $\mathbf{b}_{\mathcal{I},i}\mathbf{v}$, and the entry $\mathbf{c}_{\mathcal{I}}[i]$ describes the gap between the ith couple of the corresponding nodes on the contact interface in the reference configuration.

The matrix $\mathsf{B}_{\mathcal{E}}$ with the rows $\mathbf{b}_{\mathcal{E},i}$ and the vector $\mathbf{c}_{\mathcal{E}}$ with the entries $\mathbf{c}_{\mathcal{E},i}$ enforce the prescribed displacements on the part of the boundary with imposed Dirichlet condition and the continuity of the displacements across the auxiliary interfaces. The continuity requires that $\mathbf{b}_{\mathcal{E},i}\mathbf{v} = \mathbf{c}_{\mathcal{E},i} = 0$, where $\mathbf{b}_{\mathcal{E},i}$ are vectors with zero entries except 1 and -1 at appropriate positions.

5. Dual formulation

Even though (6) represents a standard convex quadratic programming problem, its formulation is not suitable for numerical solution. The reasons are that the stiffness matrix $\widetilde{\mathsf{S}}$ is typically ill-conditioned, singular, and the feasible set is in general so complex that projections into it can hardly be effectively computed. Under these circumstances, it would be very difficult to achieve fast identification of the active set at the solution and fast solution of the auxiliary linear problems.

The complications mentioned above may be essentially reduced by applying the duality theory of convex programming (see, e.g., Dostál [12]). The Lagrangian associated with problem (6) is given as

$$L(\mathbf{v}, \boldsymbol{\lambda}_{\mathcal{I}}, \boldsymbol{\lambda}_{\mathcal{E}}) := \frac{1}{2}\mathbf{v}^{\top}\widetilde{\mathsf{S}}\mathbf{v} - \widetilde{\mathbf{r}}^{\top}\mathbf{v} + \boldsymbol{\lambda}_{\mathcal{I}}^{\top}(\mathsf{B}_{\mathcal{I}}\mathbf{v} - \mathbf{c}_{\mathcal{I}}) + \boldsymbol{\lambda}_{\mathcal{E}}^{\top}(\mathsf{B}_{\mathcal{E}}\mathbf{v} - \mathbf{c}_{\mathcal{E}}),$$

where $\boldsymbol{\lambda}_{\mathcal{I}}$ and $\boldsymbol{\lambda}_{\mathcal{E}}$ are the Lagrange multipliers associated with the inequalities and equalities, respectively. Introducing the notation

$$\boldsymbol{\lambda} := \begin{pmatrix} \boldsymbol{\lambda}_{\mathcal{I}} \\ \boldsymbol{\lambda}_{\mathcal{E}} \end{pmatrix}, \quad \mathsf{B} := \begin{pmatrix} \mathsf{B}_{\mathcal{I}} \\ \mathsf{B}_{\mathcal{E}} \end{pmatrix}, \quad \text{and} \quad \mathbf{c} := \begin{pmatrix} \mathbf{c}_{\mathcal{I}} \\ \mathbf{c}_{\mathcal{E}} \end{pmatrix},$$

one can write the Lagrangian briefly as

$$L(\mathbf{v}, \boldsymbol{\lambda}) = \frac{1}{2}\mathbf{v}^{\top}\widetilde{\mathsf{S}}\mathbf{v} - \widetilde{\mathbf{r}}^{\top}\mathbf{v} + \boldsymbol{\lambda}^{\top}(\mathsf{B}\mathbf{v} - \mathbf{c}).$$

It is well-known [12] that (6) is equivalent to the following saddle point problem

$$L(\mathbf{u}, \overline{\boldsymbol{\lambda}}) = \sup_{\boldsymbol{\lambda}_{\mathcal{I}} \geq \mathbf{0}} \inf_{\mathbf{v}} L(\mathbf{v}, \boldsymbol{\lambda}). \tag{8}$$

For a fixed $\boldsymbol{\lambda}$, the Lagrange function $L(\cdot, \boldsymbol{\lambda})$ is convex in the first variable and the minimizer $\mathbf{u}$ of $L(\cdot, \boldsymbol{\lambda})$ satisfies

$$\widetilde{\mathsf{S}}\mathbf{u} - \widetilde{\mathbf{r}} + \mathsf{B}^{\top}\boldsymbol{\lambda} = \mathbf{0}. \tag{9}$$

Equation (9) has a solution if and only if

$$\widetilde{\mathbf{r}} - \mathsf{B}^\top \boldsymbol{\lambda} \in \mathrm{Im}\widetilde{\mathsf{S}}, \tag{10}$$

which can be expressed more conveniently by means of a full column matrix R whose columns span the null space of $\widetilde{\mathsf{S}}$ as

$$\mathsf{R}^\top(\widetilde{\mathbf{r}} - \mathsf{B}^\top \boldsymbol{\lambda}) = \mathbf{0}.$$

Recall that the blocks $\widetilde{\mathsf{S}}_p$ of $\widetilde{\mathsf{S}}$ are positive semi-definite with the known kernel of the dimension six. Thus the matrix R may be formed directly by using any basis of the rigid body modes of the subdomains, i.e.,

$$\mathsf{R} := \begin{pmatrix} \mathsf{R}_1 & \mathsf{O} & \mathsf{O} \\ \mathsf{O} & \ddots & \mathsf{O} \\ \mathsf{O} & \mathsf{O} & \mathsf{R}_s \end{pmatrix}, \quad \text{where} \quad \mathsf{R}_p := \begin{pmatrix} \mathbf{1} & \mathbf{0} & \mathbf{0} & -\mathbf{x}_2^p & \mathbf{0} & \mathbf{x}_3^p \\ \mathbf{0} & \mathbf{1} & \mathbf{0} & \mathbf{x}_1^p & -\mathbf{x}_3^p & \mathbf{0} \\ \mathbf{0} & \mathbf{0} & \mathbf{1} & \mathbf{0} & \mathbf{x}_2^p & -\mathbf{x}_1^p \end{pmatrix} \in \mathbb{R}^{3M^p \times 6},$$

and $\mathbf{x}_i^p$ is a vector of the ith coordinates of all nodes located on Γ^p.

Now assume that $\boldsymbol{\lambda}$ satisfies (10) and denote by $\widetilde{\mathsf{S}}^+$ any left generalized inverse matrix to $\widetilde{\mathsf{S}}$, i.e.,

$$\widetilde{\mathsf{S}}\widetilde{\mathsf{S}}^+\widetilde{\mathsf{S}} = \widetilde{\mathsf{S}}.$$

Note that if we denote by $\widetilde{\mathsf{S}}_p^+$ a left generalized inverse to $\widetilde{\mathsf{S}}_p$, then the matrix

$$\widetilde{\mathsf{S}}^+ := \begin{pmatrix} \widetilde{\mathsf{S}}_1^+ & \mathsf{O} & \mathsf{O} \\ \mathsf{O} & \ddots & \mathsf{O} \\ \mathsf{O} & \mathsf{O} & \widetilde{\mathsf{S}}_s^+ \end{pmatrix}$$

is a left generalized inverse to $\widetilde{\mathsf{S}}$. The action of $\widetilde{\mathsf{S}}^+$ may be evaluated at the cost comparable with that of Cholesky's decomposition applied to the regularized $\widetilde{\mathsf{S}}$ [24, 12, 8]. It may be verified directly that if $\mathbf{u}$ solves (9), then there is a vector $\boldsymbol{\alpha}$ such that

$$\mathbf{u} = \widetilde{\mathsf{S}}^+(\widetilde{\mathbf{r}} - \mathsf{B}^\top \boldsymbol{\lambda}) + \mathsf{R}\boldsymbol{\alpha}. \tag{11}$$

After substituting expression (11) into problem (8), changing the signs, and omitting the constant term, we get that $\boldsymbol{\lambda}$ solves the minimization problem

$$\text{minimize} \quad \Theta(\boldsymbol{\lambda}) \quad \text{subject to} \quad \boldsymbol{\lambda}_{\mathcal{I}} \geq \mathbf{0} \quad \text{and} \quad \widetilde{\mathsf{G}}\boldsymbol{\lambda} = \widetilde{\mathbf{e}}, \tag{12}$$

where

$$\Theta(\boldsymbol{\lambda}) := \frac{1}{2}\boldsymbol{\lambda}^\top \mathsf{F}\boldsymbol{\lambda} - \boldsymbol{\lambda}^\top \widetilde{\mathbf{d}}$$

and

$$\mathsf{F} := \mathsf{B}\widetilde{\mathsf{S}}^{+}\mathsf{B}^\top, \quad \widetilde{\mathbf{d}} := \mathsf{B}\widetilde{\mathsf{S}}^{+}\widetilde{\mathbf{r}} - \mathbf{c}, \quad \widetilde{\mathsf{G}} := \mathsf{R}^\top \mathsf{B}^\top, \quad \widetilde{\mathbf{e}} := \mathsf{R}^\top \widetilde{\mathbf{r}}.$$

Once the solution $\overline{\boldsymbol{\lambda}}$ of (12) is known, the solution $\mathbf{u}$ of (6) may be evaluated by (11) with

$$\boldsymbol{\alpha} = (\mathsf{R}^\top \widetilde{\mathsf{B}}^\top \widetilde{\mathsf{B}}\mathsf{R})^{-1}\mathsf{R}^\top \widetilde{\mathsf{B}}^\top (\widetilde{\mathbf{c}} - \widetilde{\mathsf{B}}\widetilde{\mathsf{S}}^{+}(\widetilde{\mathbf{r}} - \mathsf{B}^\top \overline{\boldsymbol{\lambda}})),$$

where

$$\widetilde{\mathsf{B}} := \begin{pmatrix} \widetilde{\mathsf{B}}_{\mathcal{I}} \\ \mathsf{B}_{\mathcal{E}} \end{pmatrix} \quad \text{and} \quad \widetilde{\mathbf{c}} := \begin{pmatrix} \widetilde{\mathbf{c}}_{\mathcal{I}} \\ \mathbf{c}_{\mathcal{E}} \end{pmatrix}$$

with the matrix $(\widetilde{\mathsf{B}}_{\mathcal{I}},\, \widetilde{\mathbf{c}}_{\mathcal{I}})$ formed by the rows of $(\mathsf{B}_{\mathcal{I}},\, \mathbf{c}_{\mathcal{I}})$ corresponding to the positive entries of $\overline{\boldsymbol{\lambda}}_{\mathcal{I}}$.

6. Preconditioning by the projector to the rigid body modes

Even though by the application of the duality in the previous section we obtained problem (12) that is much more suitable for computations than (6) and was used for efficient solution of contact problems [14], further improvement may be achieved by adapting some simple observations and the results of Farhat, Mandel, and Roux [25].

Let T denote a non–singular matrix that defines the orthonormalization of the rows of $\widetilde{\mathsf{G}}$, so that the matrix

$$\mathsf{G} := \mathsf{T}\widetilde{\mathsf{G}}$$

satisfies $\mathsf{G}\mathsf{G}^\top = \mathsf{I}$, where I denotes a unit matrix. After putting $\mathbf{e} := \mathsf{T}\widetilde{\mathbf{e}}$, problem (12) reads

$$\text{minimize} \quad \Theta(\boldsymbol{\lambda}) \quad \text{subject to} \quad \boldsymbol{\lambda}_{\mathcal{I}} \geq \mathbf{0} \quad \text{and} \quad \mathsf{G}\boldsymbol{\lambda} = \mathbf{e}. \tag{13}$$

Next we shall transform the problem of minimization on the subset of the affine space to that on the subset of the vector space by means of arbitrary $\widetilde{\boldsymbol{\lambda}}$ that satisfies

$$\mathsf{G}\widetilde{\boldsymbol{\lambda}} = \mathbf{e}.$$

Having such a $\widetilde{\boldsymbol{\lambda}}$, we can look for the solution of (13) in the form $\boldsymbol{\lambda} = \boldsymbol{\mu} + \widetilde{\boldsymbol{\lambda}}$.

A natural choice for $\widetilde{\boldsymbol{\lambda}}$ is the least squares solution of $\mathsf{G}\boldsymbol{\lambda} = \mathbf{e}$ given by

$$\widetilde{\boldsymbol{\lambda}} = \mathsf{G}^\top \mathbf{e}.$$

Though this choice of $\widetilde{\boldsymbol{\lambda}}$ works well in practical applications, it turns out that it is difficult to find a feasible initial approximation which is not too far from the solution. To avoid solving this rather theoretical problem and to simplify the reference to the relevant optimality results for the quadratic programming algorithms, we shall use in our analysis $\widetilde{\boldsymbol{\lambda}}$ which satisfies an additional inequality $\widetilde{\boldsymbol{\lambda}}_{\mathcal{I}} \geq \mathbf{0}$. To see that such a $\widetilde{\boldsymbol{\lambda}}$ exists, it is enough to notice that the feasible set of the minimization problem (13) is non–empty. We can find it effectively using the algorithms of Section 7 by the solution of the non–linear least square problem

$$\text{minimize} \quad \frac{1}{2}\|\boldsymbol{\lambda}\|^2 \quad \text{subject to} \quad \boldsymbol{\lambda}_{\mathcal{I}} \geq \mathbf{0} \quad \text{and} \quad \mathsf{G}\boldsymbol{\lambda} = \mathbf{e}. \tag{14}$$

If problem (6) is coercive, then the following lemma shows that we can even find a $\widetilde{\boldsymbol{\lambda}}$ such that $\widetilde{\boldsymbol{\lambda}}_{\mathcal{I}} = \mathbf{0}$.

Lemma 6.1 [5] *Let problem* (6) *be coercive and* $\mathsf{G} = (\mathsf{G}_{\mathcal{I}}, \mathsf{G}_{\mathcal{E}})$. *Then* $\mathsf{G}_{\mathcal{E}}$ *is a full row rank matrix and*

$$\widetilde{\boldsymbol{\lambda}} := \begin{pmatrix} \mathbf{0}_{\mathcal{I}} \\ \mathsf{G}_{\mathcal{E}}^{\top}(\mathsf{G}_{\mathcal{E}}\mathsf{G}_{\mathcal{E}}^{\top})^{-1}\mathbf{e} \end{pmatrix}$$

satisfies $\widetilde{\boldsymbol{\lambda}}_{\mathcal{I}} = \mathbf{0}$ *and* $\mathsf{G}\widetilde{\boldsymbol{\lambda}} = \mathbf{e}$.

Since we put $\boldsymbol{\lambda} = \boldsymbol{\mu} + \widetilde{\boldsymbol{\lambda}}$, it holds

$$\Theta(\boldsymbol{\lambda}) = \frac{1}{2}\boldsymbol{\lambda}^{\top}\mathsf{F}\boldsymbol{\lambda} - \boldsymbol{\lambda}^{\top}\widetilde{\mathbf{d}} = \frac{1}{2}\boldsymbol{\mu}^{\top}\mathsf{F}\boldsymbol{\mu} - \boldsymbol{\mu}^{\top}(\widetilde{\mathbf{d}} - \mathsf{F}\widetilde{\boldsymbol{\lambda}}) + \frac{1}{2}\widetilde{\boldsymbol{\lambda}}^{\top}\mathsf{F}\widetilde{\boldsymbol{\lambda}} - \widetilde{\boldsymbol{\lambda}}^{\top}\widetilde{\mathbf{d}},$$

and we can consider (in minimization) the dual function Θ without the last two constant terms. Now we can return to the old notation and reformulate problem (13) equivalently as:

$$\text{minimize} \quad \Xi_0(\boldsymbol{\lambda}) \quad \text{subject to} \quad \boldsymbol{\lambda}_{\mathcal{I}} \geq \boldsymbol{\ell}_{\mathcal{I}} := -\widetilde{\boldsymbol{\lambda}}_{\mathcal{I}} \quad \text{and} \quad \mathsf{G}\boldsymbol{\lambda} = \mathbf{0}, \tag{15}$$

where

$$\Xi_0(\boldsymbol{\lambda}) := \frac{1}{2}\boldsymbol{\lambda}^{\top}\mathsf{F}\boldsymbol{\lambda} - \boldsymbol{\lambda}^{\top}\mathbf{d}$$

and $\mathbf{d} := \widetilde{\mathbf{d}} - \mathsf{F}\widetilde{\boldsymbol{\lambda}}$.

Our final step is based on the observation that problem (15) is equivalent to

$$\text{minimize} \quad \Xi(\boldsymbol{\lambda}) \quad \text{subject to} \quad \boldsymbol{\lambda}_{\mathcal{I}} \geq \boldsymbol{\ell}_{\mathcal{I}} \quad \text{and} \quad \mathsf{G}\boldsymbol{\lambda} = \mathbf{0}, \tag{16}$$

where

$$\Xi(\boldsymbol{\lambda}) := \frac{1}{2}\boldsymbol{\lambda}^\top(\mathsf{PFP} + \rho\mathsf{Q})\boldsymbol{\lambda} - \boldsymbol{\lambda}^\top\mathsf{P}\mathbf{d},$$

ρ is a positive penalty factor, and

$$\mathsf{Q} := \mathsf{G}^\top\mathsf{G} \quad \text{and} \quad \mathsf{P} := \mathsf{I} - \mathsf{Q}.$$

denote the orthogonal projectors on the image space of $\mathsf{G}^\top$ and on the kernel of G, respectively. For convenience, let us denote the Hessian matrix of Ξ by

$$\mathcal{H} := \mathsf{PFP} + \rho\mathsf{Q}.$$

Let us note that if $[a,\, b] \subset \mathbb{R}_+$ is an interval containing non–zero elements of the spectrum $\sigma\{\mathsf{PFP}\}$ of PFP, then $\sigma\{\mathcal{H}\} \subset [a,\, b] \cup \{\rho\}$, so that $\mathcal{H}$ is non–singular. In our numerical experiments we use $\rho \approx b$. The regularization term is introduced in order to simplify the reference to the results of quadratic programming that assume regularity of the Hessian matrix of the quadratic form. Problem (16) turns out to be a suitable starting point for the development of an efficient algorithm for variational inequalities due to the classical estimates of the extreme eigenvalues. To formulate them, we shall denote by $\lambda_{\min}(\mathsf{A})$ and $\lambda_{\max}(\mathsf{A})$ the smallest and the largest eigenvalues of a given symmetric matrix A, respectively.

Theorem 6.1. *Let there be constants $b, B > 0$ independent of the discretization parameter h and the decomposition parameter H such that*

$$b \le \lambda_{\min}(\mathsf{BB}^\top) \le \lambda_{\max}(\mathsf{BB}^\top) \le B$$

and let the elements and the subdomains have regular shape and size. Then there are constants $c, C > 0$ independent of the discretization parameter h and the decomposition parameter H such that

$$c \le \lambda_{\min}(\mathsf{PFP}\,|\,\operatorname{Im}\mathsf{P}) \le \|\mathsf{PFP}\| \le C\frac{H}{h},$$

where $\mathsf{PFP}\,|\,\operatorname{Im}\mathsf{P}$ stands for the linear operator PFP defined on the image of P.

The proof of the above theorem in [6] is based on the similar bounds on spectrum formulated for the FETI case by Farhat, Mandel, and Roux [25] and on the observation of Langer and Steinbach [38] that the boundary element stiffness matrix $\widetilde{\mathsf{S}}_p$ is spectrally equivalent to some Schur complement of the corresponding finite element stiffness matrix.

Theorem 6.1 states that if we refine the mesh and increase the number of subdomains so that the ratio H/h is kept constant, we have still the same upper bound on the spectral condition number of $\mathsf{PFP} \,|\, \operatorname{Im} \mathsf{P}$. Langer and Steinbach [38] give stronger polylogarithmic bounds for the preconditioned F, but we cannot use their result since such preconditioning transforms the bound constraints to more general ones.

Example 6.1 As an example of the system of bodies in mutual contact that admits the decompositions and discretizations satisfying the assumptions of Theorem 6.1, let us consider a cuboid filled with identical cubes of the size H_0. After optionally removing some cubes and forming the bodies by "gluing" some adjacent cubes, we get the system of bodies in mutual contact that can be decomposed with the decomposition and discretization parameters H and h, $H_0/H \in \mathbb{N}$, $H/h \in \mathbb{N}$, respectively, and satisfies the assumptions of Theorem 6.1. See Figure 5 for the illustration.

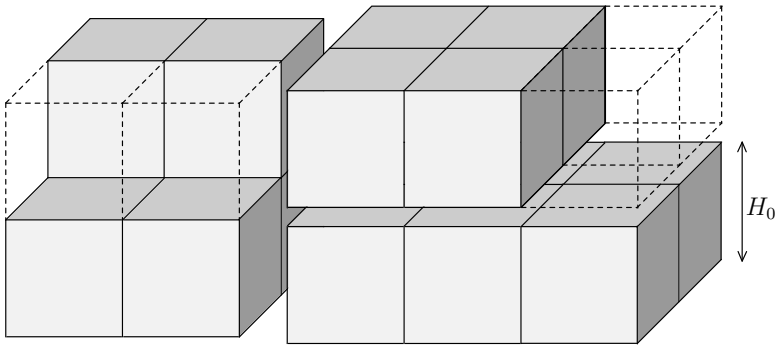

Figure 5: Example of a decomposition satisfying the assumptions of Theorem 6.1.

7. Optimal solvers to bound and equality constrained problems

For convenience of the reader, let us briefly review our algorithms for the efficient solution of the bound and equality constrained problem (16) that we use in our numerical experiments. They combine our semi-monotonic augmented Lagrangian method [13, 12], which generates approximations for the Lagrange multipliers for the equality constraints in the outer loop with the working set algorithm for the bound constrained auxiliary problems in the inner loop [21]. If a new Lagrange multiplier vector $\boldsymbol{\mu}$ is used for the equality constraints, the augmented Lagrangian for problem (16) reads

$$L(\boldsymbol{\lambda}, \boldsymbol{\mu}, \rho) := \Xi(\boldsymbol{\lambda}) + \boldsymbol{\mu}^\top \mathsf{G}\boldsymbol{\lambda}.$$

The gradient of the augmented Lagrangian L with respect to the first variable is then given by

$$\mathbf{g}(\boldsymbol{\lambda}, \boldsymbol{\mu}, \rho) := \nabla_{\boldsymbol{\lambda}} L(\boldsymbol{\lambda}, \boldsymbol{\mu}, \rho) = (\mathsf{PFP} + \rho \mathsf{Q})\, \boldsymbol{\lambda} - \mathsf{Pd} + \mathsf{G}^{\top} \boldsymbol{\mu}.$$

Recall that $\mathcal{I}$ and $\mathcal{E}$ denote the sets of the indices corresponding to the inequalities and equalities, respectively. The *projected gradient* $\mathbf{g}^P = \mathbf{g}^P(\boldsymbol{\lambda}, \boldsymbol{\mu}, \rho)$ of L at $\boldsymbol{\lambda}$ is then given component-wise by

$$\mathbf{g}_i^P := \begin{cases} \mathbf{g}_i & \text{for} \quad \boldsymbol{\lambda}_i > \boldsymbol{\ell}_i \quad \text{and} \quad i \in \mathcal{I}, \quad \text{or} \quad i \in \mathcal{E}, \\ \mathbf{g}_i^- & \text{for} \quad \boldsymbol{\lambda}_i = \boldsymbol{\ell}_i \quad \text{and} \quad i \in \mathcal{I}, \end{cases}$$

where $\mathbf{g}_i^- := \min\{\mathbf{g}_i, 0\}$ and $\boldsymbol{\ell}_i$ are the entries of $\boldsymbol{\ell}_{\mathcal{I}}$. Our algorithm is a variant of the SMALBE algorithm introduced by Dostál [13]. Our algorithm differs from SMALBE in that it keeps the penalty factor constant and, instead, it decreases the parameter M which controls the precision of the inner loop solution.

Algorithm 7.1. [12] Semi-monotonic augmented Lagrangian method for bound and equality constrained problems with update of M (**SMALBE-M**).

Step 0: {*Initialization.*}
Choose $\eta > 0,\ \beta > 1,\ M_0 > 0,\ \rho > 0,\ \boldsymbol{\mu}^0$, set $k := 0$.

Step 1: {*Inner iteration with adaptive precision control.*}
Find $\boldsymbol{\lambda}^k$ such that $\boldsymbol{\lambda}_{\mathcal{I}}^k \geq \boldsymbol{\ell}_{\mathcal{I}}$ and
$\|\mathbf{g}^P(\boldsymbol{\lambda}^k, \boldsymbol{\mu}^k, \rho)\| \leq \min\{M_k \|\mathsf{G}\boldsymbol{\lambda}^k\|, \eta\}$.

Step 2: {*Stopping criterion.*}
If $\|\mathbf{g}^P(\boldsymbol{\lambda}^k, \boldsymbol{\mu}^k, \rho)\|$ and $\|\mathsf{G}\boldsymbol{\lambda}^k\|$ are sufficiently small, then
$\boldsymbol{\lambda}^k$ is the solution.

Step 3: {*Update of the Lagrange multipliers.*}
$\boldsymbol{\mu}^{k+1} := \boldsymbol{\mu}^k + \rho \mathsf{G}\boldsymbol{\lambda}^k$

Step 4: {*Update of the balancing parameter M.*}
If $k > 0$ and $L(\boldsymbol{\lambda}^k, \boldsymbol{\mu}^k, \rho) < L(\boldsymbol{\lambda}^{k-1}, \boldsymbol{\mu}^{k-1}, \rho) + \rho \|\mathsf{G}\boldsymbol{\lambda}^k\|^2/2$,
then
$M_{k+1} := M_k/\beta$,
else
$M_{k+1} := M_k$.

Step 5: Set $k := k + 1$ and return to *Step 1.*

All the necessary parameters are listed in *Step 0*. *Step 1* may be implemented by any algorithm for minimization of the augmented Lagrangian L with respect to $\boldsymbol{\lambda}$ subject to $\boldsymbol{\lambda}_{\mathcal{I}} \geq \boldsymbol{\ell}_{\mathcal{I}}$ which guarantees convergence of the projected gradient to zero. More about the properties and implementation of SMALBE-M and closely related SMALBE algorithms may be found in [13, 12].

The unique feature of the SMALBE and SMALBE-M algorithms is their capability to find an approximate solution of problem (16) in a number of steps which is uniformely bounded in terms of bounds on the spectrum of the Hessian $\mathcal{H}$ of L. To get a bound on the number of matrix–vector multiplications, it is necessary to have an algorithm which can solve the problem

$$\text{minimize} \quad L(\boldsymbol{\lambda}, \boldsymbol{\mu}, \rho) \quad \text{with respect to} \quad \boldsymbol{\lambda} \quad \text{subject to} \quad \boldsymbol{\lambda}_{\mathcal{I}} \geq \boldsymbol{\ell}_{\mathcal{I}} \tag{17}$$

with the rate of convergence in terms of a norm of the projected gradient and in terms of the bounds on the spectrum of $\mathcal{H}$.

To describe such an algorithm, let us recall that the unique solution $\overline{\boldsymbol{\lambda}} = \overline{\boldsymbol{\lambda}}(\boldsymbol{\mu}, \rho)$ of (17) satisfies the Karush–Kuhn–Tucker (KKT) conditions [12]

$$\mathbf{g}^P(\overline{\boldsymbol{\lambda}}, \boldsymbol{\mu}, \rho) = \mathbf{0}.$$

Let $\mathcal{A}(\boldsymbol{\lambda})$ and $\mathcal{F}(\boldsymbol{\lambda})$ denote the *active set* and *free set* of indices of $\boldsymbol{\lambda}$, respectively, i.e.,

$$\mathcal{A}(\boldsymbol{\lambda}) := \{i \in \mathcal{I} : \ \boldsymbol{\lambda}_i = \boldsymbol{\ell}_i\} \quad \text{and} \quad \mathcal{F}(\boldsymbol{\lambda}) := \{i : \ \boldsymbol{\lambda}_i > \boldsymbol{\ell}_i \ \text{ or } \ i \in \mathcal{E}\}.$$

To enable an alternative reference to the KKT conditions [12], let us define the *free gradient* $\boldsymbol{\varphi}(\boldsymbol{\lambda})$ and the *chopped gradient* $\boldsymbol{\beta}(\boldsymbol{\lambda})$ by

$$\boldsymbol{\varphi}_i(\boldsymbol{\lambda}) := \begin{cases} \mathbf{g}_i(\boldsymbol{\lambda}) & \text{for} \quad i \in \mathcal{F}(\boldsymbol{\lambda}), \\ 0 & \text{for} \quad i \in \mathcal{A}(\boldsymbol{\lambda}), \end{cases} \quad \text{and} \quad \boldsymbol{\beta}_i(\boldsymbol{\lambda}) := \begin{cases} 0 & \text{for} \quad i \in \mathcal{F}(\boldsymbol{\lambda}), \\ \mathbf{g}_i^-(\boldsymbol{\lambda}) & \text{for} \quad i \in \mathcal{A}(\boldsymbol{\lambda}), \end{cases}$$

so that the KKT conditions are satisfied if and only if the projected gradient

$$\mathbf{g}^P(\boldsymbol{\lambda}) = \boldsymbol{\varphi}(\boldsymbol{\lambda}) + \boldsymbol{\beta}(\boldsymbol{\lambda})$$

is equal to zero. We call $\boldsymbol{\lambda}$ *feasible* if $\boldsymbol{\lambda}_i \geq \boldsymbol{\ell}_i$ for $i \in \mathcal{I}$. The projection P to the set of feasible vectors is defined for any $\boldsymbol{\lambda}$ by

$$P(\boldsymbol{\lambda})_i := \begin{cases} \max\{\boldsymbol{\lambda}_i, \boldsymbol{\ell}_i\} & \text{for } i \in \mathcal{I}, \\ \boldsymbol{\lambda}_i & \text{for } i \in \mathcal{E}. \end{cases}$$

Let us recall that $\mathcal{H}$ denotes the Hessian of L with respect to $\boldsymbol{\lambda}$. The *expansion step* is defined by

$$\boldsymbol{\lambda}^{k+1} := P\left(\boldsymbol{\lambda}^k - \overline{\alpha}\boldsymbol{\varphi}(\boldsymbol{\lambda}^k)\right)$$

with the steplength $\overline{\alpha} \in (0,\, 2\,\|\mathcal{H}\|^{-1}]$. This step may expand the current active set. To describe it without P, let $\widetilde{\boldsymbol{\varphi}}(\boldsymbol{\lambda})$ be the *reduced free gradient* for any feasible $\boldsymbol{\lambda}$, with entries

$$\widetilde{\boldsymbol{\varphi}}_i = \widetilde{\boldsymbol{\varphi}}_i(\boldsymbol{\lambda}) := \min\left\{\frac{\boldsymbol{\lambda}_i - \boldsymbol{\ell}_i}{\overline{\alpha}}, \boldsymbol{\varphi}_i\right\} \quad \text{for } i \in \mathcal{I}, \quad \widetilde{\boldsymbol{\varphi}}_i := \boldsymbol{\varphi}_i \quad \text{for } i \in \mathcal{E}$$

such that

$$P\left(\boldsymbol{\lambda} - \overline{\alpha}\boldsymbol{\varphi}(\boldsymbol{\lambda})\right) = \boldsymbol{\lambda} - \overline{\alpha}\widetilde{\boldsymbol{\varphi}}(\boldsymbol{\lambda}).$$

If the inequality

$$\|\boldsymbol{\beta}(\boldsymbol{\lambda}^k)\|^2 \le \Gamma_{Prop}^2 \widetilde{\boldsymbol{\varphi}}(\boldsymbol{\lambda}^k)^\top \boldsymbol{\varphi}(\boldsymbol{\lambda}^k) \tag{18}$$

holds for a parameter $\Gamma_{Prop} > 0$, then we call the iterate $\boldsymbol{\lambda}^k$ *strictly proportional*. The test (18) is used to decide which component of the projected gradient $\mathbf{g}^P(\boldsymbol{\lambda}^k)$ will be reduced in the next step.

The *proportioning step* is defined by

$$\boldsymbol{\lambda}^{k+1} := \boldsymbol{\lambda}^k - \alpha_{CG}\boldsymbol{\beta}(\boldsymbol{\lambda}^k).$$

The steplength α_{CG} is chosen to minimize $L(\boldsymbol{\lambda}^k - \alpha\boldsymbol{\beta}(\boldsymbol{\lambda}^k), \boldsymbol{\mu}^k, \rho)$ with respect to α, i.e.,

$$\alpha_{CG} := \frac{\boldsymbol{\beta}(\boldsymbol{\lambda}^k)^\top \mathbf{g}(\boldsymbol{\lambda}^k)}{\boldsymbol{\beta}(\boldsymbol{\lambda}^k)^\top \mathcal{H}\boldsymbol{\beta}(\boldsymbol{\lambda}^k)}.$$

The purpose of the proportioning step is to remove indices from the active set.

The *conjugate gradient step* is defined by

$$\boldsymbol{\lambda}^{k+1} := \boldsymbol{\lambda}^k - \alpha_{CG}\mathbf{p}^k, \quad \alpha_{CG} := \frac{(\mathbf{p}^k)^\top \mathbf{g}(\boldsymbol{\lambda}^k)}{(\mathbf{p}^k)^\top \mathcal{H}\mathbf{p}^k},$$

where $\mathbf{p}^k$ is the conjugate gradient direction [27, 12] which is constructed recurrently. The recurrence starts (or restarts) with $\boldsymbol{p}^s := \boldsymbol{\varphi}(\boldsymbol{\lambda}^s)$ whenever $\boldsymbol{\lambda}^s$ is generated by the expansion step or the proportioning step. If $\mathbf{p}^k$ is known, then $\mathbf{p}^{k+1}$ is given by the formulae [27, 12]

$$\mathbf{p}^{k+1} := \boldsymbol{\varphi}(\boldsymbol{\lambda}^{k+1}) - \gamma\mathbf{p}^k, \quad \gamma := \frac{\boldsymbol{\varphi}(\boldsymbol{\lambda}^{k+1})^\top \mathcal{H}\mathbf{p}^k}{(\mathbf{p}^k)^\top \mathcal{H}\mathbf{p}^k}.$$

The conjugate gradient steps are used to carry out the minimization in the face

$$\mathcal{W}_{\mathcal{J}} := \{\boldsymbol{\lambda} :\ \boldsymbol{\lambda}_i = \boldsymbol{\ell}_i \quad \text{for } i \in \mathcal{J}\}, \quad \mathcal{J} := \mathcal{A}(\boldsymbol{\lambda}^s),$$

efficiently. The algorithm that we use may now be described as follows.

Algorithm 7.2. [21, 12] Modified proportioning with reduced gradient projections (**MPRGP**).

Choose $\boldsymbol{\lambda}^0$ such that $\boldsymbol{\lambda}^0_i \geq \boldsymbol{\ell}_i$ for $i \in \mathcal{I}$, $\overline{\alpha} \in (0, 2\|\mathcal{H}\|^{-1}]$, and $\Gamma_{Prop} > 0$, set $k := 0$.

For $k \geq 0$ and $\boldsymbol{\lambda}^k$ known, choose $\boldsymbol{\lambda}^{k+1}$ by the following rules:

i) If $\mathbf{g}^P(\boldsymbol{\lambda}^k) = \mathbf{0}$, then set $\boldsymbol{\lambda}^{k+1} := \boldsymbol{\lambda}^k$.

ii) If $\boldsymbol{\lambda}^k$ is strictly proportional and $\mathbf{g}^P(\boldsymbol{\lambda}^k) \neq \mathbf{0}$, then try to generate $\boldsymbol{\lambda}^{k+1}$ by the conjugate gradient step. If $\boldsymbol{\lambda}^{k+1}_i \geq \boldsymbol{\ell}_i$ for $i \in \mathcal{I}$, then accept it, else generate $\boldsymbol{\lambda}^{k+1}$ by the expansion step.

iii) If $\boldsymbol{\lambda}^k$ is not strictly proportional, define $\boldsymbol{\lambda}^{k+1}$ by proportioning.

For $\overline{\alpha} \in (0, 2\|\mathcal{H}\|^{-1})$, the MPRGP algorithm has an R-linear rate of convergence of both $\boldsymbol{\lambda}^k$ and $\mathbf{g}^P(\boldsymbol{\lambda}^k)$ in terms of the spectral condition number of the Hessian $\mathcal{H}$ of L [11, 12]. For more details about the properties and implementation of the MPRGP algorithm, we refer to [21, 12].

8. Optimality

To show that Algorithm 7.1 (SMALBE-M) with the inner loop implemented by Algorithm 7.2 (MPRGP) is optimal for the solution of problem (16) with $\boldsymbol{\ell}_{\mathcal{I}} := -\widetilde{\boldsymbol{\lambda}}_{\mathcal{I}} \leq \mathbf{0}$, we introduce a new notation that complies with that used in [13]. We use

$$\mathcal{T} := \{(H, h) \in \mathbb{R}^2 : \ H \leq 1, \ 2h \leq H, \ \text{and} \ H/h \in \mathbb{N}\}$$

as the set of indices. Given a constant $C \geq 2$, let us define a subset $\mathcal{T}_C$ of $\mathcal{T}$ by

$$\mathcal{T}_C := \{(H, h) \in \mathcal{T} : \ H/h \leq C\}.$$

For any $t \in \mathcal{T}$, we define

$$\begin{array}{lll} \mathsf{A}_t := \mathcal{H} = \mathsf{PFP} + \rho\mathsf{Q}, & \mathbf{b}_t := \mathsf{P}\mathbf{d}, & \\ \mathsf{C}_t := \mathsf{G}, & \boldsymbol{\ell}_{t,\mathcal{I}} := \boldsymbol{\ell}_{\mathcal{I}}, & \boldsymbol{\ell}_{t,\mathcal{E}} := -\infty \end{array}$$

by the vectors and matrices generated with the discretization and decomposition parameters H and h, respectively, so that problem (16) is equivalent to the problem

$$\text{minimize} \quad \Xi_t(\boldsymbol{\lambda}_t) \quad \text{subject to} \quad \mathsf{C}_t\boldsymbol{\lambda}_t = \mathbf{0} \quad \text{and} \quad \boldsymbol{\lambda}_t \geq \boldsymbol{\ell}_t \tag{19}$$

with

$$\Xi_t(\boldsymbol{\lambda}_t) := \frac{1}{2}\boldsymbol{\lambda}_t^\top \mathsf{A}_t \boldsymbol{\lambda}_t - \mathbf{b}_t^\top \boldsymbol{\lambda}_t.$$

By using these definitions and $\mathsf{G}\mathsf{G}^\top = \mathsf{I}$, we get

$$\|\mathsf{C}_t\| \leq 1 \quad \text{and} \quad \|\boldsymbol{\ell}_t^+\| = 0, \tag{20}$$

where for any vector $\mathbf{v}$ with the entries $\mathbf{v}_i$ we define a vector $\mathbf{v}^+$ by $\mathbf{v}_i^+ := \max\{\mathbf{v}_i, 0\}$. Moreover, it follows by Theorem 6.1 that for any $C \geq 2$ there are constants $a_{\max}^C \geq a_{\min}^C > 0$ such that

$$a_{\min}^C \leq \lambda_{\min}(\mathsf{A}_t) \leq \lambda_{\max}(\mathsf{A}_t) \leq a_{\max}^C \tag{21}$$

for any $t \in \mathcal{T}_C$. Furthermore, there are positive constants C_1 and C_2 such that $a_{\min}^C \geq C_1$ and $a_{\max}^C \leq C_2 C$. In particular, it follows that the assumptions of Theorem 5 (i.e., the relations in (20) and (21)) of [13] are satisfied for any set of indices $\mathcal{T}_C$, $C \geq 2$, so that we have the following result:

Theorem 8.1 [12, 13] *Let $C \geq 2$ and $\varepsilon > 0$ denote given constants, let $\{\boldsymbol{\lambda}_t^k\}, \{\boldsymbol{\mu}_t^k\}$, and $\{M_{t,k}\}$ be generated by Algorithm 7.1 (SMALBE-M) for* (19) *with*

$$\|\boldsymbol{b}_t\| \geq \eta_t > 0, \ \beta > 1, \ M_{t,0} := M_0 > 0, \ \rho > 0, \ \text{and} \ \boldsymbol{\mu}_t^0 := 0.$$

Let $s \geq 0$ denote the smallest integer such that

$$\beta^{2s}\rho \geq M_0^2 / a_{\min}^C$$

and assume that Step 1 of Algorithm 7.1 is implemented by means of Algorithm 7.2 (MPRGP) with parameters

$$\Gamma_{Prop} > 0 \quad \text{and} \quad \overline{\alpha} \in (0, 2/a_{\max}^C),$$

so that it generates the iterates $\boldsymbol{\lambda}_t^{k,0}, \boldsymbol{\lambda}_t^{k,1}, \ldots, \boldsymbol{\lambda}_t^{k,l} =: \boldsymbol{\lambda}_t^k$ for the solution of (19) *starting from $\boldsymbol{\lambda}_t^{k,0} := \boldsymbol{\lambda}_t^{k-1}$ with $\boldsymbol{\lambda}_t^{-1} := \mathbf{0}$, where $l = l_{t,k}$ is the first index satisfying*

$$\|\mathbf{g}^P(\boldsymbol{\lambda}_t^{k,l}, \boldsymbol{\mu}_t^k, \rho)\| \leq M_{t,k}\|\mathsf{C}_t \boldsymbol{\lambda}_t^{k,l}\|$$

or

$$\|\mathbf{g}^P(\boldsymbol{\lambda}_t^{k,l}, \boldsymbol{\mu}_t^k, \rho)\| \leq \varepsilon\|\mathbf{b}_t\| \quad \text{and} \quad \|\mathsf{C}_t \boldsymbol{\lambda}_t^{k,l}\| \leq \varepsilon\|\mathbf{b}_t\|.$$

Then for any $t \in \mathcal{T}_C$ and problem (19)*, Algorithm 7.1 generates an approximate solution $\boldsymbol{\lambda}_t^{k_t}$ which satisfies*

$$\|\mathbf{g}^P(\boldsymbol{\lambda}_t^{k_t}, \boldsymbol{\mu}_t^{k_t}, \rho)\| \leq \varepsilon\|\mathbf{b}_t\| \quad \text{and} \quad \|\mathsf{C}_t \boldsymbol{\lambda}_t^{k_t}\| \leq \varepsilon\|\mathbf{b}_t\|$$

at $\mathcal{O}(1)$ matrix–vector multiplications by the Hessian of the augmented Lagrangian for (19) *and*

$$M_{t,k} \geq M_0/\beta^s.$$

9. Numerical experiments

Described algorithms are implemented within the MatSol library [36] developed in the Matlab environment and tested on the solution of two benchmarks comprising 3D multibody frictionless contact problems. In the first benchmark, we varied the decomposition and discretization parameters H and h, respectively, in order to demonstrate the scalability of our method. In the second one, we illustrate the ability to solve real world problems. For all computations we used an HP Blade system, model BLc7000 with one master node and eight computational nodes, each with two dual core CPUs AMD Opteron 2210 HE. The maximum number of parallel processes was limited by 24 due to the number of available licences of Matlab Distributed Computing Engine which was used as the parallel programming environment.

For the evaluation of all boundary element matrices, we used the quadrature formulae proposed by Sauter and Schwab [49]. The corresponding routines were implemented in ANSI C and consequently linked to the MatSol library through the Matlab MEX interface.

All tests were carried out with the following SMALBE-M parameters:

$$\rho \approx \|\mathsf{PFP}\|, \quad M_0 := 1, \quad \beta := 10, \quad \eta := \|\mathsf{P}\mathbf{d}\|, \quad \boldsymbol{\mu}^0 := \mathbf{0}.$$

The computation of ρ was realized by several iterations of Rayleigh's quotients. More hints on the choice of parameters can be found in [12]. The stopping criterion was chosen as

$$\max\{\|\mathbf{g}^P(\boldsymbol{\lambda}^k, \boldsymbol{\mu}^k, \rho)\|, \ \|\mathsf{G}\boldsymbol{\lambda}^k\|\} \leq 10^{-4}\|\mathsf{P}\mathbf{d}\|.$$

The MPRGP algorithm always used the parameters

$$\overline{\alpha} := \frac{2}{\rho}, \quad \Gamma_{Prop} := 1.$$

9.1. 3D Hertz problem

Our first benchmark is a variant of the well-known 3D Hertz problem, which models the pressure distribution between an elastic sphere and an elastic half-space in mutual contact. In Figure 6, we see quarters of both bodies due to the symmetry with respect to the x_1x_3 and x_2x_3 planes. The lower body is made of aluminium with $E^1 := 7 \cdot 10^4$ [MPa] and $\nu^1 := 0.35$ and the upper body is made of steel with $E^2 := 2.1 \cdot 10^5$ [MPa] and $\nu^2 := 0.29$. The upper body is pressed down by the imposed vertical boundary traction $-2,000$ [N/mm^2] which acts only along the top face, the rest of Γ_n^2 is free. The lower body remains free along the whole Γ_n^1. The symmetry condition is imposed on all corresponding Dirichlet boundaries and the lower body is fixed

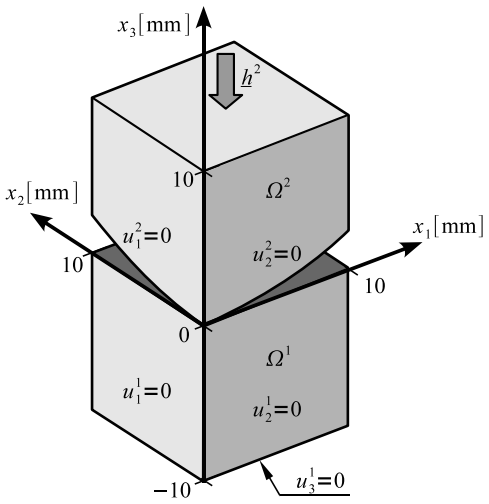

Figure 6: Geometry of the considered 3D Hertz problem.

vertically along its bottom face. The linearized non-interpenetration condition (4) is imposed between the bodies.

Both bodies were decomposed into subdomains whose boundaries were discretized by triangular grids. We tested both uniform and non-uniform (METIS) domain decompositions. The initial and deformed states with the traces of the non-uniform decomposition into 16 subdomains and $h := 1$ are depicted in Figures 7 and 8, respectively, and the corresponding normal contact traction on Γ_c^1 can be seen in Figure 9. Note that in Figure 9 we can see a mesh dependency of the computed traction; with a smaller h we obtain a smoother result.

To demonstrate the numerical scalability of our method, we kept $H/h = 8$. Table 1 shows the results for the uniform domain decomposition and we can see that the number of matrix–vector multiplications grows only moderately, in agreement with the theory. Table 2 reports the results obtained for the METIS domain decomposition and we observe that the number of the Hessian multiplications increases significantly for large decompositions due to irregular shapes of the subdomains. Let us note that the total number of MPRGP iterations is always lower than the total number of multiplications by the Hessian.

The parallel scalability of our algorithm for the uniform and METIS domain decompositions can be seen in Table 3. In the parallel scalability tests, we fixed the discretization parameter to $h := 10/16$ and increased the number of partitions into subdomains accordingly to the number of used CPUs.

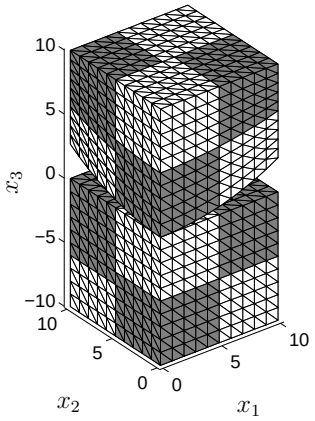

Figure 7: Initial state.

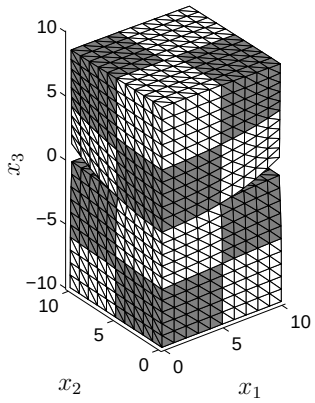

Figure 8: Deformed state.

number of subdomains	4	16	64	256	512	1,024
number of processors	4	16	24	24	24	24
primal variables	4,632	18,528	74,112	296,448	592,896	1,185,792
dual variables	1,260	7,248	33,312	145,920	300,224	617,088
defect	24	96	384	1,536	3,072	6,144
Hessian multiplications	104	121	226	361	385	281
SMALBE-M iterations	13	16	12	12	13	14
solver time [s]	6	12	52	301	718	2,129
total time [s]	32	47	166	835	1,806	4,858

Table 1: Numerical scalability for the uniform domain decomposition.

number of subdomains	4	16	64	256	512	1,024
number of processors	4	16	24	24	24	24
primal variables	6,024	18,936	84,756	344,616	664,824	1,332,070
dual variables	1,830	7,476	39,318	172,902	342,444	700,140
defect	24	96	384	1,536	3,072	6,144
Hessian multiplications	100	128	216	617	645	1,390
SMALBE-M iterations	10	17	10	7	8	6
solver time [s]	7	13	62	651	1,407	7,906
total time [s]	52	49	213	1,341	2,671	10,717

Table 2: Performance for the METIS domain decomposition.

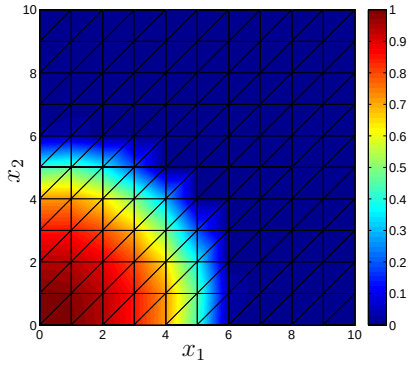

Figure 9: The normal contact traction [10^4 N/mm^2] on Γ_c^1.

	uniform		METIS	
number of CPUs	solver	total	solver	total
2	45	844	40	853
4	39	318	37	319
8	15	102	15	98
16	11	45	12	49

Table 3: Solver and total times [s] illustrating the parallel scalability.

9.2. Real world problem: ball bearing

Now let us present the performance of our algorithm on a real world multibody contact problem without friction. We consider the analysis of the stress in the ball bearing depicted in Figure 10, where the outer part of the outer ring is fixed and the inner part of the inner ring is under the traction. This problem is difficult since the traction acting on the lower part of the inner ring is distributed throughout the non-linear interface of the cage and balls to the fixed outer ring. The ball bearing was decomposed into 960 subdomains using METIS, see Figure 11. The computed solution (the normal contact traction) of the problem discretized by 1,071,759 primal and 470,258 dual variables can be seen in Figures 12 and 13. To obtain the solution, we needed 1,843 matrix–vector multiplications. The solver and total times are equal to 6,070 and 7,632 seconds, respectively. Note that within the solution process, we had to identify 11,250 active constraints.

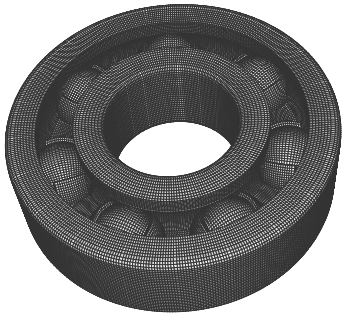

Figure 10: The ball bearing geometry with generated mesh.

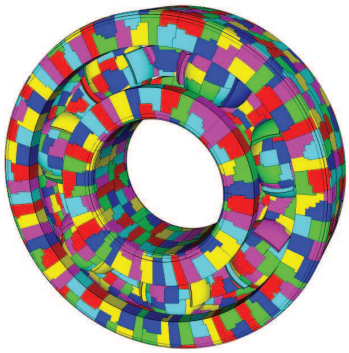

Figure 11: Decomposition into 960 non-uniform subdomains.

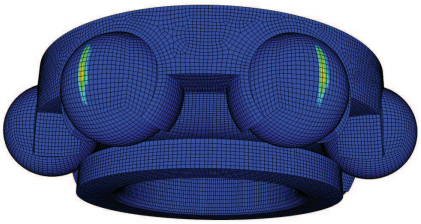

Figure 12: Computed normal contact traction.

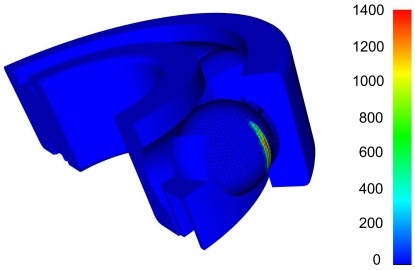

Figure 13: Detail of the computed normal contact traction; the units are [N/mm^2].

10. Comments and conclusions

We have presented the scalability results related to the application of the Total BETI based domain decomposition method with the natural coarse grid preconditioning and of our recently developed algorithms for the solution of bound and equality constrained convex quadratic programming problems to the solution of 3D multibody contact problems of elastostatics without friction. In particular, we have shown that an approximate solution of the discretized elliptic variational inequality which describes the equilibrium of a system of elastic bodies in mutual contact may be obtained in a number of matrix–vector multiplications bounded independently of the discretization parameter provided the ratio of the decomposition and the discretization parameters is kept bounded.

Numerical experiments with the academic benchmark are in agreement with the theory. The efficiency of the algorithm for the solution of the frictionless contact problems has been demonstrated also on a real world problem. We have documented also the parallel scalability inherited from the basic BETI scheme. The solution of auxiliary linear problems in the inner loop may be improved by standard preconditioners [53].

Acknowledgements

This research has been financially supported by the grants GA CR 201/07/0294 and the Ministry of Education of the Czech Republic No. MSM6198910027.

References

[1] Avery, P., Rebel, G., Lesoinne, M., Farhat, C.: A numerically scalable dual–primal substructuring method for the solution of contact problems – part I: the frictionless case. Comput Methods Appl Mech Eng **193**, 2403–2426 (2004)

[2] Avery P, Farhat C.: The FETI family of domain decomposition methods for inequality-constrained quadratic programming: Application to contact problems with conforming and nonconforming interfaces. Computer Methods in Applied Mechanics and Engineering, 198(21-26):1673-1683, 2009.

[3] Bebendorf, M.: Hierarchical Matrices: A Means to Efficiently Solve Elliptic Boundary Value Problems. Lecture Notes in Computational Science and Engineering (LNCSE) **63**, Springer - Verlag (2008)

[4] Bebendorf, M., Rjasanow. S.: Adaptive lowrank approximation of collocation matrices. Computing **70**, 1–24 (2003)

[5] Bouchala, J., Dostál, Z., Sadowská, M.: Scalable Total BETI based algorithm for 3D coercive contact problems of linear elastostatics. Computing **85**, 189–217 (2009)

[6] Bouchala, J., Dostál, Z., Sadowská, M.: Theoretically supported scalable BETI method for variational inequalities. Computing **82**, 53–75 (2008)

[7] Bouchala, J., Dostál, Z., Sadowská, M.: Scalable BETI for Variational Inequalities. Lecture Notes in Computational Science and Engineering – selection of 71 refereed papers presented at the 17th International Conference on Domain Decomposition Methods, Springer – Verlag Berlin Heidelberg, 167–174 (2008)

[8] Brzobohatý, T., Dostál, Z., Kovář, P., Kozubek, T., Markopoulos, A.: Cholesky–SVD decomposition with fixing nodes to stable evaluation of a generalized inverse of the stiffness matrix of a floating structure. Submitted.

[9] Burczyňski, T., Adamczyk, T.: The boundary element formulation for multiparameter structural shape optimization. Appl Math Model **9**, 195–200 (1985)

[10] Costabel, M.: Boundary integral operators on Lipschitz domains: Elementary results. SIAM J Math Anal **19**, 613–626 (1988)

[11] Dostál, Z., Domorádová, M., Sadowská, M.: Superrelaxation in minimizing quadratic functions subject to bound constraints. Comput Optim Appl (2009). Published online, DOI: 10.1007/s10589-009-9237-6

[12] Dostál, Z.: Optimal Quadratic Programming Algorithms with Applications to Variational Inequalities. 1st edition, SOIA 23, Springer US, New York (2009)

[13] Dostál, Z.: An optimal algorithm for bound and equality constrained quadratic programming problems with bounded spectrum. Computing **78**, 311–328 (2006)

[14] Dostál, Z., Friedlander, A., Santos, S.A.: Solution of coercive and semicoercive contact problems by FETI domain decomposition. Contemporary Mathematics **218**, 82–93 (1998)

[15] Dostál, Z., Friedlander, A., Santos, S.A., Malík, J.: Analysis of semicoercive contact problems using symmetric BEM and augmented Lagrangians. Eng Anal Bound Elem **18**, 195–201 (1996)

[16] Dostál, Z., Kozubek, T., Vondrák, V., Brzobohatý, T., Markopoulos, A.: Scalable TFETI algorithm for the solution of multibody contact problems of elasticity. Int J Numer Meth Eng (2009). Published online, DOI: 10.1002/nme.2807

[17] Dostál, Z., Kozubek, T., Horyl, P., Brzobohatý, T., Markopoulos, A.: Scalable TFETI algorithm for two dimensional multibody contact problems with friction. Accepted in J Comput Appl Math.

[18] Dostál, Z., Kozubek, T., Markopoulos, A., Brzobohatý, T., Vondrák, V., Horyl, P.: Theoretically supported scalable TFETI algorithm for the solution of multibody 3D contact problems with friction. Submitted.

[19] Dostál, Z., Horák, D.: Theoretically supported scalable FETI for numerical solution of variational inequalities. SIAM J Numer Anal **45**, 500–513 (2007)

[20] Dostál, Z., Horák, D., Kučera, R.: Total FETI – an easier implementable variant of the FETI method for numerical solution of elliptic PDE. Commun Numer Meth En **22**, 1155–1162 (2006)

[21] Dostál, Z., Schöberl, J.: Minimizing Quadratic Functions Subject to Bound Constraints with the Rate of Convergence and Finite Termination. Comput Optim Appl **30**, 23–43 (2005)

[22] Dureisseix, D., Farhat, C.: A numerically scalable domain decomposition method for solution of frictionless contact problems. Int J Numer Meth Eng **50**, 2643–2666 (2001)

[23] Eck, C., Steinbach, 0., Wendland, W.L.: A symmetric boundary element method for contact problems with friction. Math Comput Simulat **50**, 43–61 (1999)

[24] Farhat, C., Géradin, M.: On the general solution by a direct method of a large scale singular system of linear equations: application to the analysis of floating structures. Int J Numer Meth Eng **41**, 675–696 (1997)

[25] Farhat, C., Mandel, J., Roux, F.-X.: Optimal convergence properties of the FETI domain decomposition method. Comput Method Appl Mech Eng **115**, 365–385 (1994)

[26] Farhat, C., Roux, F.-X.: A method of finite element tearing and interconnecting and its parallel solution algorithm. Int J Numer Meth Eng **32**, 1205–1227 (1991)

[27] Golub, G.H., Van Loan, C.F.: Matrix Computation. The John Hopkins Univ. Press, Baltimore, 1985.

[28] Greengard, L.F., Rokhlin, V.: A new version of the fast multipole method for the Laplace equation in three dimensions. Acta numerica, Cambridge University Press, 229–269 (1997)

[29] Greengard, L.F., Rokhlin, V.: A fast algorithm for particle simulations. J Comput Phys **73**, 325-48 (1987)

[30] Han, H.: The boundary integro–differential equations of three–dimensional Neumann problem in linear elasticity. Numer Math **68**, 269–281 (1994)

[31] Hlaváček, I., Haslinger, J., Nečas, J., Lovíšek, J.: Solution of Variational Inequalities in Mechanics. Springer - Verlag Berlin (1988)

[32] Iontcheva, A.H., Vassilevski, P.S.: Monotone multigrid methods based on element agglomeration coarsening away from the contact boundary for the Signorini's problem. Numer Linear Algebra Appl **11**, 189–204 (2004).

[33] Kikuchi, N., Oden, J.T.: Contact Problems in Elasticity. SIAM - Philadelphia (1988)

[34] Kornhuber, R.: Adaptive monotone multigrid methods for nonlinear variational problems. Teubner - Verlag: Stuttgart (1997)

[35] Kornhuber, R., Krause, R.: Adaptive multigrid methods for Signorini's problem in linear elasticity. Comput Visual Sci **4**, 9–20 (2001)

[36] Kozubek, T., Markopoulos, A., Brzobohatý, T., Kučera, R., Vondrák, V., Dostál, Z.: MatSol – MATLAB effcient solvers for problems in engineering. http://www.am.vsb.cz/matsol

[37] Kupradze, V.D., Gegelia, T.G., Baseleisvili, M.O., Burculadze, T.V.: Three-dimensional problems of the mathematical theory of elasticity and thermoelasticity. North-Holland Series in Applied Mathematics and Mechanics, vol. 25, Amsterdam, New York, Oxford: North-Holland Publishing Company (1979)

[38] Langer, U., Steinbach, O.: Boundary element tearing and interconnecting methods. Computing **71**, 205–228 (2003)

[39] Langer, U., Pechstein, C.: Coupled FETI/BETI solvers for nonlinear potential problems in (un)bounded domains. In Proceedings of the SCEE 2006 (ed. by Gabriela Ciuprina and Daniel Ioan), Mathematics in Industry, vol. 11, Springer – Verlag Heidelberg, 371–377 (2007)

[40] McLean, W.: Strongly Elliptic Systems and Boundary Integral Equations. Cambridge University Press (2000)

[41] Liu, Y., Nishimura, N.: The fast multipole boundary element method for potential problems: A tutotial. Eng Anal Bound Elem **30**, 371-381 (2006)

[42] Schöberl, J.: Solving the Signorini problem on the basis of domain decomposition techniques. Computing **60**, 323–344 (1998)

[43] Maischak, M., Stephan, E.P.: Adaptive hp-versions of BEM for Signorini problems. Applied Numerical Mathematics archive **54**, 425–449 (2005)

[44] Of, G.: The All-floating BETI Method: Numerical Results. Lecture Notes in Computational Science and Engineering – selection of 71 refereed papers presented at the 17th International Conference on Domain Decomposition Methods, Springer – Verlag Berlin Heidelberg, 295–302 (2008)

[45] Of, G., Steinbach, O.: The all-floating boundary element tearing and interconnecting method. J Numer Math **17**, 4, pp 277–298 (2009)

[46] Of, G., Steinbach, O., Wendland, W.L.: Applications of a fast multipole Galerkin in boundary element method in linear elastostatics, Comput Visual Sci **8**, 201–209 (2005)

[47] Rjasanow, S., Steinbach, O.: The Fast Solution of Boundary Integral Equations. Mathematical and Analytical Techniques with Applications to Engineering, Springer - New York (2007)

[48] Sadowská, M.: Scalable Total BETI for 2D and 3D Contact Problems. Ph.D. Thesis, VŠB - Technical University of Ostrava, http://www.am.vsb.cz/sadowska/publikace (2008)

[49] Sauter, S., Schwab, C.: Randelementmethoden - Analyse, Numerik und Implementierung schneller Algorithmen. Teubner - Verlag (2004). In German.

[50] Steinbach, O.: Fast evaluation of Newton potentials in boundary element methods. East-West J Numer Math **7**, 211–222 (1999)

[51] Steinbach, O.: Stability Estimates for Hybrid Coupled Domain Decomposition Methods. Lecture Notes in Mathematics 1809, Springer - Verlag Berlin Heidelberg (2003)

[52] Steinbach, O.: Numerical Approximation Methods for Elliptic Boundary Value Problems. Finite and Boundary Elements. Springer - New York (2008)

[53] Toselli, A., Widlund, O.B.: Domain Decomposition Methods - Algorithms and Theory. Springer - Verlag Berlin Heidelberg (2005)

[54] Wohlmuth, B.I., Krause, R.: Monotone methods on nonmatching grids for nonlinear contact problems. SIAM J Sci Comput **25**, 324–347 (2003)

[55] Wriggers, P.: Contact Mechanics. Springer - Berlin (2005)